Research Article

Differential Micronucleus Frequency in Isogenic Human Cells Deficient in DNA Repair Pathways Is a Valuable Indicator for Evaluating Genotoxic Agents and Their Genotoxic Mechanisms

Liton Kumar Saha,[1] Sujin Kim,[2] Habyeong Kang,[2] Salma Akter,[1]
Kyungho Choi,[2] Tetsushi Sakuma,[3] Takashi Yamamoto,[3]
Hiroyuki Sasanuma,[1] Kouji Hirota,[4] Jun Nakamura,[5]
Masamitsu Honma,[6] and Shunichi Takeda[1]*

[1]Department of Radiation Genetics, Kyoto University, Graduate School of Medicine, Yoshida Konoe, Sakyo-ku, Kyoto, 606-8501, Japan
[2]Department of Environmental Health, School of Public Health, Seoul National University,599 Gwanak-ro, Gwanak-gu, Seoul, 151-742, Korea
[3]Department of Mathematical and Life Sciences, Graduate School of Science, Hiroshima University, Higashi-Hiroshima, 739-8526, Japan
[4]Department of Chemistry, Tokyo Metropolitan University, Minami-Osawa, Hachioji, Tokyo, 192-0397, Japan
[5]Department of Laboratory Animal Science, School of Veterinary Science, Osaka Prefecture University, Rinku Ourai Kita, Izumisano, Osaka, 598-8531, Japan
[6]Division of Genetics and Mutagenesis, National Institute of Health Sciences, 1-18-1 Kamiyoga, Setagaya-ku, Tokyo, 158-8501, Japan

The micronucleus (MN) test has become an attractive tool both for evaluating the genotoxicity of test chemicals because of its ability to detect clastogenic and aneugenic events and for its convenience. As the MN assay has been mostly performed using only DNA repair-proficient mammalian cells, we believed that the comparison of the MN frequency between DNA repair-proficient and -deficient human cells may be an excellent indicator for detecting the genotoxic potential of test chemicals and for understanding their mode of action. To address this issue, the following five genes encoding DNA-damage-response (DDR) factors were disrupted in the TK6 B cell line, a human cell line widely used for the MN test: *FANCD2*, *DNA polymerase* ζ (*REV3*), *XRCC1*, *RAD54*, and/or *LIG4*. Using these isogenic TK6 cell lines, the MN test was conducted for four widely-used DNA-damaging agents: methyl methanesulfonate (MMS), hydrogen peroxide (H_2O_2), γ-rays, and mitomycin C (MMC). The frequency of micronuclei in the double strand break repair-deficient $RAD54^{-/-}/LIG4^{-/-}$ cells after exposure to γ-rays, H_2O_2, MMS and MMC was 6.2-7.5 times higher than that of parental *wild-type* TK6 cells. The percentages of cells exhibiting micronuclei in the base excision repair- and single strand break repair-deficient $XRCC1^{-/-}$ cells after exposure to H_2O_2, MMC and MMS were all $\sim$5 times higher than those of *wild-type* cells. In summary, a supplementary MN assay using the combination of $RAD54^{-/-}/LIG4^{-/-}$, $XRCC1^{-/-}$ and *wild-type* TK6 cells is

---

a promising method for detecting the genotoxic potential of test chemicals and their mode of action. Environ. Mol. Mutagen. 59:529–538, 2018. © 2018 Wiley Periodicals, Inc.

INTRODUCTION

A great number of new chemicals are being synthesized and registered every year; thus, a convenient *in vitro* assay is needed for assessing their genotoxicity and understanding the details of their action. Currently, the induction of DNA damage in mammalian cells by physical and chemical agents is evaluated by a number of short-term *in vitro* genotoxicity bioassays, including those that measure the frequency of gene mutations, chromosomal aberrations, and micronuclei [Yamamoto et al., 2011]. The *in vitro* micronucleus (MN) test has become an attractive tool for genotoxicity testing because of its capacity to detect not only clastogenic and aneugenic events but also because of its simplicity in scoring, accuracy, wide applicability in different cell types, and amenability to automation. The OECD guideline 487 for the MN test was recently made available, and it refers to the extensive data supporting the validity of the assay using various rodent cell lines (CHO, V79, CHL and L5178Y) and human cell lines such as TK6 [OECD, 2014]. The human lymphoblastoid TK6 cell line has been widely used for several *in vitro* genotoxicity tests including the MN test [Liber and Thilly, 1982; Olive et al., 1993; Greenwood et al., 1998; Amundson et al., 2005; Hastwell et al., 2009]. For the *in vitro* MN assay, DNA-repair-proficient cells have been routinely utilized; however, one major issue with the current method is that these cells can quickly and accurately repair DNA damage before the bioassay can detect any positive genotoxic outcomes. Therefore, we posited that comparing MN frequency between DNA-repair-proficient and -deficient cells could be a valuable indicator to detect the genotoxic potential of various chemicals and physical agents and their mode of action.

In the current study, we applied the usage of isogenic DNA-repair-deficient human cell lines to the *in vitro* MN test. To generate isogenic DNA-repair-deficient clones, we chose the TK6 cells as a parental cell line because these cells express functional p53 similarly to normal human tissues [Honma and Hayashi, 2011], rapidly proliferate (13 hrs per cycle), and are very sensitive to genotoxic chemicals. The rapid proliferation of these cells makes them susceptible to substantial fractions of lesions induced by genotoxic chemicals that interfere with DNA replication, leading to MN formation particularly in cells deficient in pathways that normally protect against responding to the interference the interference of DNA replication. We generated $RAD54^{-/-}/LIG4^{-/-}$, $XRCC1^{-/-}$, $FANCD2^{-/-}$, and $REV3^{-/-}$ TK6 cells by gene disruption (Tables I and II) as these five DDR factors cover a wide range of proteins important in the event of DNA lesions. The disrupted genes include FANCD2 for interstrand crosslink repair, DNA polymerase zeta (REV3) for trans-lesion DNA synthesis (TLS), and XRCC1 for base excision repair and single-strand break (SSB) repair, leading to the generation of $FANCD2^{-/-}$, $REV3^{-/-}$, and $XRCC1^{-/-}$ cells. We also simultaneously disrupted two genes involved in double-strand break (DSB) repair and generated $RAD54^{-/-}/LIG4^{-/-}$ cells. Additionally, we included $XPA^{-/-}$ cells in this study to cover all possible DDR pathways in humans; XPA is an essential protein in the nucleotide excision repair pathway to repair bulky DNA adducts caused by UV and intrastrand crosslink agents. The frequency of MN in these mutant cells was then compared to that of the parental TK6 cells after exposure to DNA-damaging agents such as mitomycin C (MMC), an inter-strand crosslinking agent; methyl methanesulfonate (MMS), an alkylating agent; hydrogen peroxide (H_2O_2); and γ-rays. MMC and MMS act by crosslinking and methylating DNA, respectively. H_2O_2 causes oxidative base damage to DNA, and γ-rays directly generate DNA double strand breaks. Among the four TK6 mutants, $RAD54^{-/-}/LIG4^{-/-}$ and $XRCC1^{-/-}$ cells showed markedly efficient induction of MNs following treatment of the four agents. In summary, we propose a supplementary MN test using the combination of $RAD54^{-/-}/LIG4^{-/-}$, $XRCC1^{-/-}$ and *wild-type* TK6 cells to measure genotoxic potential as well as to investigate the mode of action of chemicals, routinely used for screening.

MATERIALS AND METHODS

Cell Line and Culture Conditions

DNA-repair-deficient TK6 cell lines (Table II) and *wild-type* cells were cultured in RPMI 1640 medium (Life Technologies, Grand Island, NY, USA) supplemented with 10% (vol/vol) heat-inactivated horse serum (Cell Culture Bioscience, Nichirei Biosciences, Inc., Tokyo, Japan), 200 μg/ml sodium pyruvate, 100 U/ml penicillin and 100 μg/ml streptomycin, in a culture flask at 37°C, 5% CO_2 and 100% humidity.

Generation of Human DNA-Repair-Deficient Human TK6 Cells

The TK6 mutants used in this study are shown in Table II. To create the mutant cells, either guide RNAs targeting the exons using the Zhang CRISPR tool [Ran et al., 2013] or TALEN expression plasmids using the Golden Gate TALEN Kit and the TAL Effector Kit (Addgene) [Cermak et al., 2011; Sakuma et al., 2013] were generated together with gene-targeting constructs carrying selection markers. Either 6 μg of the CRISPR plasmid or a pair of TALEN expression plasmids and 2 μg of each of the two gene-targeting vectors carrying different selection marker genes were transfected into 4×10^6 TK6 cells using the Neon

Environmental and Molecular Mutagenesis. DOI 10.1002/em

MN Assay Using Isogenic TK6 B Cells Deficient in DNA Repair   531

TABLE I. DNA-Damage-Response Factors and Their Functions

DNA-damage-response factor	Function	Reference
DNA polymerase ζ (REV3)	TLS	Hochegger et al. [2004]
FANCD2	Fanconi-anemia interstrand crosslink repair	Kim and D'Andrea [2012]
Ligase 4 (LIG4)	DSB repair by NHEJ	Goodarzi and Jeggo [2013]
RAD54	DSB repair by HR	Holthausen et al. [2010]
XRCC1	Base excision repair and SSB repair	Horton et al. [2008]
XPA	Nucleotide excision repair	Musich et al. [2017]

TLS = Translesion DNA synthesis, FANCD2= Fanconi anemia group D2 protein, NHEJ = Non-homologous end joining, HR = Homologous recombination, DSB = Double strand break, SSB = Single strand break, RAD54 = Radiation damage protein 54, XRCC1= X-ray repair cross-complementing protein 1, XPA= Xeroderma Pigmentosum, Complementation Group A.

TABLE II. Panel of Isogenic Mutant TK6 Cells

Genotype	Marker genes	Type of genome editing techniques	References
$REV3^{-/-}$	$puro^R$, neo^R	TALEN	This study
$XRCC1^{-/-}$	bsr^R, his^R	TALEN	This study
$FANCD2^{-/-}$	$puro^R$, neo^R	CRISPR/Cas9	This study
$RAD54^{-/-}/LIG4^{-/-}$	$puro^R$, neo^R, $hygro^R$	CRISPR/Cas9 and TALEN	This study
$RAD54^{-/-}$	$puro^R$, neo^R	TALEN	Keka et al. [2015]
$LIG4^{-/-}$	$puro^R$, neo^R	CRISPR/Cas9	Keka et al. [2015]
$XPA^{-/-}$	$puro^R$, $hygro^R$	CRISPR/Cas9	Mohiuddin et al. [2018]

*TSCER2 is derived from the TK6 cell line and carries a marker gene for measuring heteroallelic recombination in the *thymidine kinase* gene [Yatagai et al., 2008].
REV3= Protein reversionless 3-like (REV3L) or DNA polymerase ζ, XRCC1= X-ray repair cross-complementing protein 1, FANCD2= Fanconi anemia group D2 protein, RAD54 = Radiation damage protein 54, LIG4 = Ligase 4, TALEN= Transcription Activator-Like Effector Nucleases, CRISPR/Cas9= Clustered Regulatory Interspaced Short Palindromic Repeats)/Cas9, XPA= Xeroderma Pigmentosum, Complementation Group A.

Transfection System (Life Technologies, US) with three 1350-volt pulses and 10 msec pulse widths. After electroporation, the cells were rested in 20 ml of drug-free medium. 48 hrs later, the cells were seeded into 96-well plates for selection for two weeks with two antibiotics against the selection marker genes in the transfected gene-targeting constructs indicated in Table II. Gene-targeting events were confirmed by western blot analysis and/or RT-PCR.

RT–PCR

The loss of *RAD54* transcript was confirmed by RT-PCR using the primers 5′-ACTGCAGCAAGTTCAGTGCC-3′ and 5′-CTCTACTAT GCTATTAGGAG-3′. The loss of *REV3* transcript was also confirmed by RT-PCR using the primers 5′- GGCGACATGTTTTCAGTAAGGAT AG-3′and 5′-GTGTCTTTCCTTCTCATGATAACCA-3′. GAPDH transcripts were analyzed as a positive control for the RT-PCR analysis using the primers 5′-CATTGCTGACAGGATGCAGAAGG-3′ and 5′-T GCTTGCTGATCCACATCTGCTGG-3′.

Western Blot

Human XRCC1 and FANCD2 were detected using the following primary antibodies: anti-XRCC1 (1/1000, mouse monoclonal, Abcam, 33-2-5:ab1838) and anti-FANCD2 (1/1000, mouse monoclonal, Santa Cruz Biotechnology Inc., F-117: sc-20022). Anti-mouse IgG conjugated with HRP (NA931, GE Healthcare) was used as a secondary antibody.

Test Chemicals and Agent

MMS, (CAS 22801-14) and H_2O_2 (CAS 081–04215) were purchased from Nacalai Tesque Inc. (Kyoto, Japan) and Wako Pure Chemical Industries, Ltd (Osaka, Japan), respectively. MMC (CAS M4287) was purchased from Sigma-Aldrich Inc. (CA, USA). All test chemicals were dissolved in phosphate-buffered saline (Takara Bio Inc., Shiga, Japan). All test chemicals were prepared immediately prior to treatment. Caesium 137 installed in a Gamma cell R40 Exactor (Best Theratronics Ltd, Ontario, Canada) was the source for gamma-ray radiation.

Colony Formation Assay

To measure the sensitivity of TK6 cell lines to genotoxic agents, a colony formation assay was conducted. The sensitivity was evaluated by counting colony formation in methylcellulose plates as described previously [Zhao et al., 2007; Qing et al., 2011]. The cells were treated with various concentrations of MMS, MMC and H_2O_2 for 4 hrs. During the treatment with MMC and H_2O_2, the cells were exposed in complete media whereas in case of MMS, the cells were exposed in serum-free media. Irradiation of the cells using a ^{137}Cs γ-ray source was done after putting the cells into 6-well cluster plates. Serially-diluted TK6 cells were then plated onto triplicated wells of 6-well cluster plates in 5 ml/well of D-MEM/F-12 (Life Technologies) supplemented with 10% horse serum, 2 mM L-Glutamine, 200 μg/ml sodium pyruvate and 1.5% (weight/vol) methylcellulose (Wako, Osaka, Japan). Colonies were counted 10–14 days after the irradiation or chemical treatment. The percentage of surviving colonies after the irradiation or chemical treatment was determined relative to the percentage of surviving untreated colonies.

Treatment with Genotoxic Agents for the MN Test

Cell density was maintained under 1.5×10^6 cells/ml. The population doubling time is ∼13 hrs for TK6 cells. Cell suspensions were prepared at 2×10^5 cells/ml and treated with serial dilutions of one of the chemicals described above for 4 hrs at 37°C or irradiated with gamma-

rays at a dosage rate of 1 Gy/min. Vehicle or serial dilutions of the chemicals (500 μl) were added to 4.95 ml of cell suspension in a 6 well plate (single cell culture). Cell suspensions (5 ml) in a 6 well plate were irradiated for 0 (control) to 1 min on ice (single cell culture).

Relative Survival Measurements for the MN Test

Cytotoxicity was evaluated by cell viability measured via trypan blue dye exclusion (TBDE) and cytostatic activity on the basis of cell growth. The TBDE assay was conducted just after the treatment (Day 0) and 2 days later (Days 0 and 2). The cells in an aliquot of the cell suspension were counted just after the treatment and on Day 2. The relative increase in cell count (RICC) for Day 2 was calculated using the following formula [Greenwood et al., 2004; Fellows et al., 2008]:

$$RICC = \frac{Increase\ in\ number\ of\ cells\ in\ treated\ cultures\ (final - starting)}{Increase\ in\ number\ of\ cells\ in\ control\ cultures\ (final - starting)}$$

Dose Selection for the MN Test

The dose that reduced the viability of individual gene-disrupted cells to 50 to 60% was selected following OECD guideline 487. TK6 mutants ($RAD54^{-/-}/LIG4^{-/-}$, $XRCC1^{-/-}$, and $REV3^{-/-}$) and *wild-type* cells were exposed to all four DNA-damaging agents. The viability of $FANCD2^{-/-}$ cells was tested only with MMC, since the FANC-deficient cells are well known to be highly sensitive to crosslinking agents [Kim and D'Andrea, 2012]. We then used the doses of the DNA-damaging agents indicated in Supporting Information, Figure 1, which caused 50% to 71% survival relative to that of non-treated cells.

MN Scoring via Microscopy

In accordance with a previously reported method [Honma and Hayashi, 2011], the micronuclei were counted at 24 and 48 hrs after treatment. A small portion of the cell culture ($\sim 1 \times 10^6$ cells) from the flask was transferred to a centrifuge tube and then centrifuged. The pellet was suspended in hypotonic 75 mM KCl solution for 10 min at room temperature, rinsed twice with ice-cold fixative (glacial acetic acid: methanol of 1:3) and then resuspended in methanol containing 1% (vol/vol) acetic acid. A drop of the suspension was placed on a clean glass slide, which was air-dried, and the cells were stained with 40 μg/ml acridine orange solution. The slides were cover-slipped, and the cells (only those showing well-outlined interphase and mononucleated cells) were immediately examined at 400x magnification under an Olympus BX50 Fluorescence Microscope (excitation: 460–490 nm, absorbing: 520 nm; Olympus Corporation, Tokyo, Japan). In total, at least three thousand cells (those exhibiting well-outlined interphase and mononucleated cells) per dose were examined (one thousand cells per replicate), and the frequency (%) of micronucleated cells was determined. The induced MN frequency was calculated by subtracting the percentage of micronucleated cells without exposure to DNA-damaging agents from that after exposure to DNA-damaging agents.

Statistical Analyses

Analysis of covariance (ANCOVA) was used to test for mean intercept differences and differences in the slopes of the linear dose-response curves in cell survival analyses between *wild-type* and a series of mutant cells using Graph Pad Prism 7. *P*-values were two-sided and adjusted for multiple comparisons, as noted. Statistical significance of the induced micronucleus frequency in the mutants at a defined dose, in comparison with that in the *wild-type*, was determined using a two-tailed t-test. The induced micronucleus frequency was calculated considering propagation of errors following the formula B − A ± (SD(a) + SD(b)), where B = MN frequency after treatment and A = MN frequency without treatment of DNA damaging agent.

RESULTS

Generation of DNA-Repair-Deficient TK6 Cell Lines

We previously generated $RAD54^{-/-}$ and $LIG4^{-/-}$ TK6 cells (Table II) [Keka et al., 2015], and here, we disrupted the $RAD54$ gene in the $LIG4^{-/-}$ TK6 cells. The genotype of the resulting $RAD54^{-/-}/LIG4^{-/-}$ TK6 cell lines was verified via RT-PCR and western blot (Fig. 1A). $XRCC1$ (Supporting Information, Fig. 2), $FANCD2$ (Supporting Information, Fig. 3), and $REV3$ (Supporting Information, Fig. 4) genes were also disrupted in TK6 cells. Inactivation of the $XRCC1$ and $FANCD2$ genes was evaluated via western blot analysis (Figs. 1B and 1C). Disruption of the $REV3$ gene was confirmed via RT-PCR (Fig. 1D).

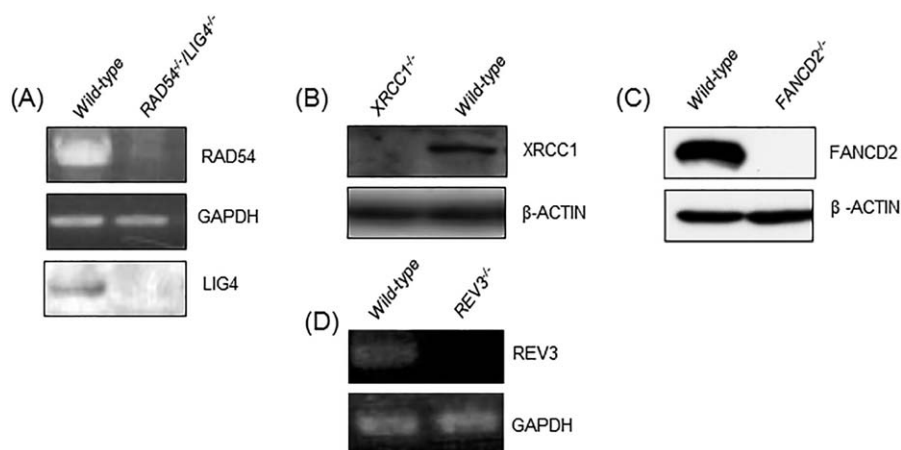### Analysis of Cellular Toxicity of DNA-Damaging Agents in the Mutant Clones

We evaluated the cell toxicity profiles of the TK6 mutant clones to γ-rays, H$_2$O$_2$, MMC and MMS using the colony formation assay. The sensitivity profiles of all of the tested mutants are shown in Figure 2. $RAD54^{-/-}/LIG4^{-/-}$ cells displayed the highest sensitivity to γ-rays followed by $RAD54^{-/-}$ and $LIG4^{-/-}$ cells (Fig. 2A). With regards to cellular sensitivity to MMS, $XRCC1^{-/-}$ cells showed the greatest sensitivity. All of the mutant lines, including $RAD54^{-/-}/LIG4^{-/-}$ cells, showed higher sensitivity to MMS than did the parental TK6 cells (Fig. 2B). $RAD54^{-/-}/LIG4^{-/-}$ cells showed the most elevated sensitivity to H$_2$O$_2$, followed by $XRCC1^{-/-}$ cells, and $RAD54^{-/-}$ and $FANCD2^{-/-}$ cells showed mild sensitivity to H$_2$O$_2$ (Fig. 2C). Following exposure to MMC, $FANCD2^{-/-}$ cells showed the most sensitivity. The $RAD54^{-/-}/LIG4^{-/-}$, $RAD54^{-/-}$ and $LIG4^{-/-}$ cells showed mild sensitivity to MMC (Fig. 2D).

MN Induction by DNA-Damaging Agents

While $RAD54^{-/-}/LIG4^{-/-}$, $XRCC1^{-/-}$, $REV3^{-/-}$ and *wild-type* cells were exposed to γ-rays, MMS, MMC and H$_2$O$_2$, $FANCD2^{-/-}$ cells were treated with MMC only. The frequency of cells displaying MNs (the MN frequency) at 48 hrs (Fig. 3) was counted, following a protocol described in previous reports [Honma and Hayashi, 2011; Kimura et al., 2013]. Some of the MN assays were also repeated at 24 hrs (Supporting Information, Fig. 5) following OECD guideline 487, which requires the measurement of MNs after 1.5 to 2 divisions following exposure of cells to DNA-damaging agents.

γ-rays: The cells were treated with γ-rays at the following levels: 0.06 Gy for $RAD54^{-/-}/LIG4^{-/-}$ (RICC: 69%), 0.13 Gy for $REV3^{-/-}$ (RICC: 55%) and 0.25 Gy for $XRCC1^{-/-}$ (RICC: 69%) (Supporting Information, Fig. 1). The *wild-type* cells were exposed to γ-rays at all three different doses to compare the MN frequency in each

Environmental and Molecular Mutagenesis. DOI 10.1002/em

MN Assay Using Isogenic TK6 B Cells Deficient in DNA Repair   533

Fig. 1. Gene disruption of TK6 cells. (**A-C**) Western blot analysis of indicated gene-disrupted TK6 clones using the antibody against the disrupted gene and (**D**) RT-PCR analysis to determine transcript levels of the gene-of-interest in the mutant and wild-type TK6 cells.
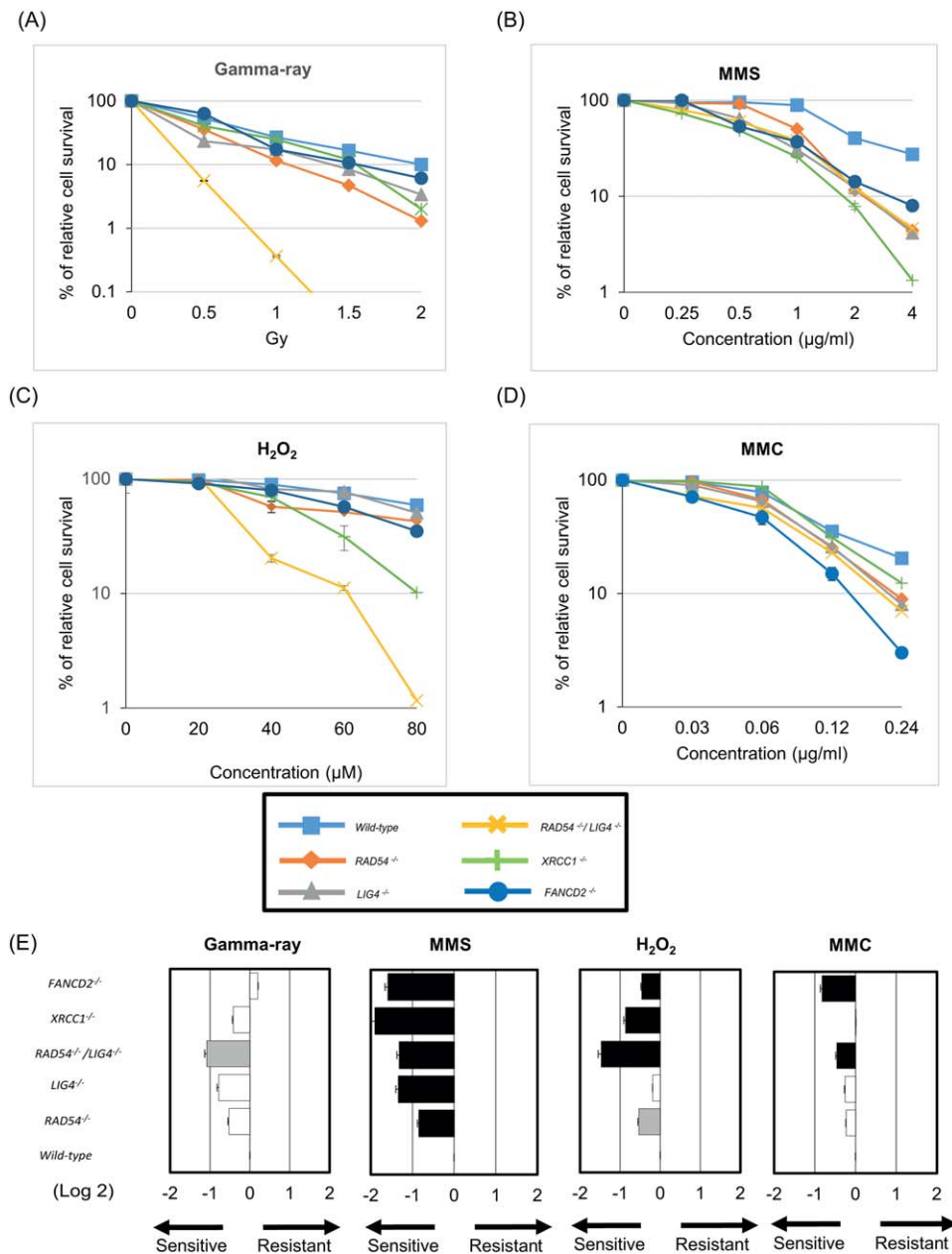
mutant (Figs. 3A, 3C, and 3E). To calculate the MN frequency induced by γ-rays, we subtracted the MN frequency in irradiated cells by that in non-irradiated cells (Subtracted values shown in Figs. 3B, 3D, and 3F). The MN frequency induced by the irradiation was 6.2, 5.3 and 4 times higher in $RAD54^{-/-}/LIG4^{-/-}$, $XRCC1^{-/-}$ and $REV3^{-/-}$ cells, respectively, when compared to *wild-type* cells. Thus, the loss of XRCC1 and REV3 increases the MN frequency to comparable extents as the simultaneous loss of the two major DSB factors, LIG4 and RAD54. The MN frequency was also measured at 24 hrs after 0.06 Gy γ-irradiation (Supporting Information, Fig. 5A). The MN frequency induced by the irradiation was 4.1 times higher in $RAD54^{-/-}/LIG4^{-/-}$ cells in comparison with *wild-type* cells (Supporting Information, Fig. 5A). We also treated the cells with a lower dose of γ-rays at the following levels: 0.03 Gy for $RAD54^{-/-}/LIG4^{-/-}$ cells (RICC: 83%) and 0.13 Gy for $XRCC1^{-/-}$ cells (RICC: 116%). The MN frequency induced by the irradiation was 5.9 and 3.9 times higher in $RAD54^{-/-}/LIG4^{-/-}$ and $XRCC1^{-/-}$ cells, respectively, when compared to *wild-type* cells (Supporting Information, Fig. 7).

H₂O₂: We exposed $RAD54^{-/-}/LIG4^{-/-}$ cells (RICC: 58%) to 5 μM H₂O₂ and also exposed $XRCC1^{-/-}$ (RICC: 80%) and $REV3^{-/-}$ (RICC: 65%) cells to 40 μM H₂O₂ (Supporting Information, Fig. 1). The *wild-type* cells were exposed to both 5 μM and 40 μM H₂O₂. We then measured the MN frequency at 48 hrs (Figs. 3A, 3C, and 3E). The subtracted MN frequency values were 6.4, 5.2, and 6.3 times higher for $RAD54^{-/-}/LIG4^{-/-}$, $XRCC1^{-/-}$ cells and $REV3^{-/-}$ cells, respectively (Figs. 3B, 3D, and 3F). The MN frequency was also evaluated at 24 hrs after treatment of $XRCC1^{-/-}$ and *wild-type* cells with 40 μM H₂O₂ (Supporting Information, Fig. 5B). The MN frequency induced by H₂O₂ was 4.9 times higher in $XRCC1^{-/-}$ cells, when compared with *wild-type* cells (Supporting Information, Fig.

5B). We also exposed $RAD54^{-/-}/LIG4^{-/-}$ cells (RICC: 65%) to 2.5 μM H₂O₂ and $XRCC1^{-/-}$ cells (RICC: 63%) to 20 μM H₂O₂. The *wild-type* cells were exposed to both 2.5 μM and 20 μM H₂O₂. The subtracted MN frequency values were 4.5 and 3.7 times higher for $RAD54^{-/-}/LIG4^{-/-}$ and $XRCC1^{-/-}$ cells respectively, in comparison with *wild-type* cells. (Supporting Information, Fig. 7)

MMS: We exposed $XRCC1^{-/-}$ (RICC: 50%) and *wild-type* cells to 250 ng/ml MMS and also exposed $RAD54^{-/-}/LIG4^{-/-}$ (RICC: 57%) and $REV3^{-/-}$ (RICC: 50%) cells to 500 ng/ml MMS (Supporting Information, Fig. 1) for measuring the MN frequency at 48 hrs. The MMS-induced MN frequency was 7.1 times higher in $RAD54^{-/-}/LIG4^{-/-}$, 5 times higher in $XRCC1^{-/-}$, and 3.6 times higher in $REV3^{-/-}$ cells, in comparison with *wild-type* cells (Figs. 3B, 3D, and 3F). The measurement of the MN frequency at 24 hrs indicates that the MMS-induced MN frequency was 5.8 times higher in $XRCC1^{-/-}$ cells when compared to *wild-type* cells (Supporting Information, Fig. 5B). We also exposed $XRCC1^{-/-}$ (RICC: 67%) and *wild-type* cells to 125 ng/ml MMS and $RAD54^{-/-}/LIG4^{-/-}$ (RICC: 57%) cells to 250 ng/ml MMS (Supporting Information, Fig. 1) to measure the MN frequency at 48 hrs. The MMS-induced MN frequency was 4.4 times higher in $RAD54^{-/-}/LIG4^{-/-}$ and 4.8 times higher in $XRCC1^{-/-}$ cells, in comparison with *wild-type* cells (Supporting Information, Fig. 7).

MMC: The MN frequency was quantitated at 48 hrs after treatment of cells with 0.06 μg/ml MMC. The RICC values were 61% for $RAD54^{-/-}/LIG4^{-/-}$, 63% for $XRCC1^{-/-}$, 51% for $REV3^{-/-}$, and 71% for $FANCD2^{-/-}$ cells (Supporting Information, Fig. 1). The MMC-induced MN frequency was 7.5 times higher in $RAD54^{-/-}/LIG4^{-/-}$, 5.5 times higher in $XRCC1^{-/-}$, 5.7 times higher in $REV3^{-/-}$ cells, and 5.3 times higher in $FANCD2^{-/-}$ cells, in comparison with *wild-type* cells (Figs. 3B, 3D, 3F, and 3H). We then measured the MN frequency at 24 hrs after treatment

Environmental and Molecular Mutagenesis. DOI 10.1002/em

534   Kumar Saha et al.

(A)

(B)

(C)

(D)

Legend:
Wild-type
RAD54⁻/⁻
LIG4⁻/⁻
RAD54⁻/⁻/ LIG4⁻/⁻
XRCC1⁻/⁻
FANCD2⁻/⁻

(E)

Fig. 2. Sensitivity of DNA-repair-deficient TK6 mutant cells to γ-rays (A), MMS (B), H₂O₂ (C), and MMC (D) as measured via colony formation assay. The error bars represent SD from three independent experiments. (E) Sensitivity profiles of the indicated DNA-damaging agents in the selected DNA repair-deficient TK6 panel. Negative (the left side) and positive (the 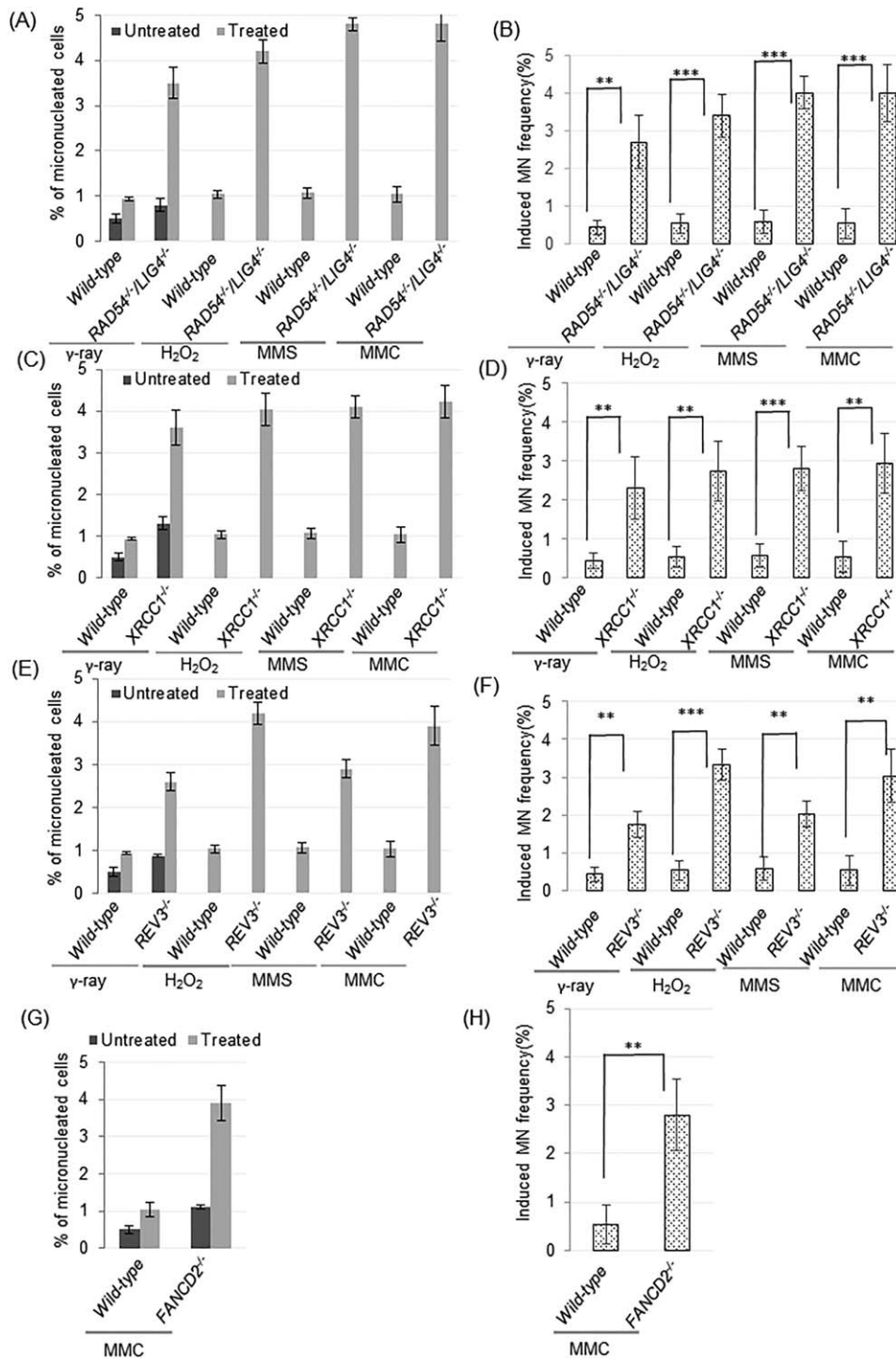right side) scores indicate that the indicated cells are sensitive and resistant to the DNA-damaging agents, respectively. *Wild-type* cells are shown at the bottom with a reference value of 0. The average IC₅₀ and standard deviations (*n* = 3) of each drug in *wild-type* cells were calculated. *P* ≤ 0.01, (black-colored bar); 0.01 < *P* < 0.05, (gray-colored bar); and not significant, (white-colored bar); in comparison with *wild-type cells* as analyzed by ANCOVA.

of *XRCC1⁻/⁻* cells with 0.06 μg/ml MMC (Supporting Information, Fig. 5A). The MMC-induced MN frequency was 6 times higher in *XRCC1⁻/⁻* cells in comparison with *wild-type* cells (Supporting Information, Fig. 5B). The MN frequency was also quantitated at 48 hrs after treatment of cells with 0.03 μg/ml MMC. The RICC values were 69% for *RAD54⁻/⁻/LIG4⁻/⁻* and 81% for *XRCC1⁻/⁻* cells. The MMC-induced MN frequency was 6.5 times

higher in *RAD54⁻/⁻/LIG4⁻/⁻* and 4 times higher in *XRCC1⁻/⁻* cells, in comparison with *wild-type* cells (Supporting Information, Fig. 7).

DISCUSSION

We prepared a panel of isogenic DNA-repair-deficient TK6 cell lines and measured the MN frequency following

Environmental and Molecular Mutagenesis. DOI 10.1002/em

MN Assay Using Isogenic TK6 B Cells Deficient in DNA Repair   535

Fig. 3. The MN test in *wild-type* and indicated DNA- repair-deficient TK6 clones at 48 hrs after treatment with indicated DNA-damaging agents. (**A**, **C**, **E**, and **G**). **B**, **D**, **F**, and **H** indicate the frequency of micronucleated cells (%) induced by the indicated DNA-damaging agents. Error bars represent SD from at least three independent experiments. $*P < 0.05$, $**P < 0.01$ and $***P < 0.001$.

exposure of the cells to four widely used DNA-damaging agents: γ-rays, H_2O_2, MMC, and MMS. All TK6 mutants tested in the present study showed markedly higher MN frequency over parental TK6 cells. The number of MNs induced by γ-rays, H_2O_2, MMS and MMC increased 6.2,

6.4, 7.1 and 7.5 times, respectively, in $RAD54^{-/-}/LIG4^{-/-}$ cells in comparison with *wild-type* cells. The number of MNs induced by γ-rays, H_2O_2, MMS and MMC all increased over 5 times in $XRCC1^{-/-}$ cells in comparison with *wild-type* cells. These results strongly suggest that

examining the differential MN frequency between iso-genic TK6 cells proficient and deficient in DNA repair pathways could be a valuable supplementary analysis to clarify the genotoxicity of presumed non-genotoxic chemicals and physical agents as well as to investigate their mode of action.

We next investigated the dose response of DNA damaging agent-treated $RAD54^{-/-}/LIG4^{-/-}$ and $XRCC1^{-/-}$ cells by performing the MN test at a dose/concentration two times lower than that at the highest RICC. We found a dose-dependent increase in the MN formation in $RAD54^{-/-}/LIG4^{-/-}$ and $XRCC1^{-/-}$ cells. $RAD54^{-/-}/LIG4^{-/-}$ cells showed a 1.6 times higher level of MN induction than $XRCC1^{-/-}$ cells at a two times lower dose of gamma-rays ($RAD54^{-/-}/LIG4^{-/-}$ cells, 6.2 times higher MN induction at 0.06 Gy vs $XRCC1^{-/-}$ cells, 3.9 times higher at 0.13 Gy, all compared to wild-type). Moreover, even at very low dose of gamma rays (0.03 Gy), $RAD54^{-/-}/LIG4^{-/-}$ cells displayed a 5.9 times higher induction of MN than wild-type cells. These MN data suggest that in order to examine and understand gamma-ray-induced genotoxicity, $RAD54^{-/-}/LIG4^{-/-}$ cells are more useful than $XRCC1^{-/-}$ cells. This observation is plausible, as gamma rays directly cause double strand break (DSB) formation to DNA, and RAD54 and LIG4 are involved in the DSB repair by HR and NHEJ pathways, respectively.

In terms of the MN induction by H_2O_2, we found that at 20 μM of H_2O_2, $XRCC1^{-/-}$ cells show an induction of MN frequency at 3.7 times higher in comparison with wild-type cells whereas even at a low dose of H_2O_2 (5 μM), induction of MN frequency in $RAD54^{-/-}/LIG4^{-/-}$ cells is 6.4 times higher in comparison with wild-type cells. Therefore, a 4-fold lower concentration of H_2O_2 can induce a 1.7 times higher level of MN in $RAD54^{-/-}/LIG4^{-/-}$ cells over $XRCC1^{-/-}$ cells. These MN data also suggest that in order to examine and understand H_2O_2-induced genotoxicity, $RAD54^{-/-}/LIG4^{-/-}$ cells may be more useful than $XRCC1^{-/-}$ cells because H_2O_2 efficiently generates single-strand breaks (SSBs) and SSBs are often converted to double-strand breaks (DSBs).

The current study demonstrates the utility of $RAD54^{-/-}/LIG4^{-/-}$ TK6 cells for detecting various DNA-damaging agents and their mode of action. The data are in agreement with the reported efficient detection of the genotoxic potential of chemicals from the National Toxicology Program chemical library using $RAD54^{-/-}/KU70^{-/-}$ chicken DT40 cells [Nishihara et al., 2016]. The clear advantage of the $RAD54^{-/-}/LIG4^{-/-}$ TK6 mutant is that they are capable of proliferating with nearly normal kinetics, show a plating efficiency (60%) comparable to wild-type cells (70%), and exhibit relatively low spontaneously arising MNs (Fig. 3A). As expected from previous studies analyzing cells deficient in both HR and NHEJ [Fukushima et al., 2001; Couëdel et al., 2004; Mills et al., 2004], the $RAD54^{-/-}/LIG4^{-/-}$ TK6 cell line is valuable for detecting

MNs caused by agents that directly generate DSBs as well as for determining their mode of action. Moreover, the increased detection of MN in $RAD54^{-/-}/LIG4^{-/-}$ cells after H_2O_2 and MMS treatment is interesting since these two agents generate DSBs with low efficiencies; instead, they have been found to induce mutagenesis and apoptosis mainly though interference of DNA replication by base damage [Hochegger et al., 2004; Branzei and Foiani, 2010]. The LIG4-dependent DSB repair pathway (NHEJ) is incapable of repairing DSBs that occur during DNA replication, such as DSBs induced by the topoisomerase I poison, camptothecin and the poison against poly[ADP ribose]polymerase, olaparib [Hochegger et al., 2006; Murai et al., 2012; Maede et al., 2014; Kobayashi et al., 2015]. In addition, RAD54 plays only a minor role in repairing DSBs that occur during DNA replication in comparison with RAD51, a factor essential for HR; as such, RAD54-deficient mice are viable while the loss of RAD51 is lethal to cells, causing numerous DSBs during DNA replication [Sonoda et al., 1998; Eppink et al., 2011]. Considering the fact that ionizing-radiation induces far more base damage and SSBs compared to DSBs [Bradley and Kohn, 1979], efficient induction of MNs in $XRCC1^{-/-}$ and $REV3^{-/-}$ cells likely reflects the important roles for REV3 and XRCC1 in preventing conversion of base damage and SSBs to DSBs and MNs through DNA replication. Further studies are required for elucidating the molecular mechanism underlying MN induction associated with H_2O_2 and MMS exposure. Based on these results, we propose that the application of $RAD54^{-/-}/LIG4^{-/-}$ TK6 cells in the conventional MN test would be significant for understanding the mode of action of genotoxic agents.

In the present study, $XRCC1^{-/-}$ and $REV3^{-/-}$ TK6 cells were created, as we expected a marked increase in the MN frequency caused by genotoxic agents that introduce base damage. In fact, $REV3^{-/-}$ chicken DT40 cells are very sensitive to a wide variety of DNA-damaging agents including tamoxifen, 4-hydroxyestradiol and nitric oxide [Mizutani et al., 2004; Wu et al., 2006]. The current study indicates that $XRCC1^{-/-}$ TK6 cells are more useful for the supplemental MN test than $REV3^{-/-}$ TK6 cells for the following reasons. 1) The plating efficiency of $XRCC1^{-/-}$ cells is better than that of $REV3^{-/-}$ cells (data not shown). 2) $XRCC1^{-/-}$ cells show a more prominent phenotype in terms of MMS-induced toxicity (Fig. 2) and MN frequency (Fig. 3) in comparison with $REV3^{-/-}$ cells. A disadvantage of $XRCC1^{-/-}$ cells is that bulky adducts, including UV-lesions, sensitize $REV3^{-/-}$ cells but not $XRCC1^{-/-}$ cells [Horton et al., 2008; Takezawa et al., 2011]. Thus, including translesion DNA synthesis- (TLS-) deficient TK6 cells other than $REV3^{-/-}$ cells in the MN assay may be recommended for determining the mode of action of a wide variety of mutagenic chemical compounds. This is because a number of TLS polymerases

Environmental and Molecular Mutagenesis. DOI 10.1002/em

MN Assay Using Isogenic TK6 B Cells Deficient in DNA Repair   537

collaboratively undergo DNA synthesis past various types of DNA lesions [Sale et al., 2012]. Moreover, TLS dominantly contributes to mutagenesis during the physiological cell cycle [Gibbs et al., 2005]. To create a TLS-deficient TK6 mutant to detect a wide variety of mutagenic potential, we need to create TK6 cells deficient in multiple TLS polymerases, as we have done for the DT40 cell line [Yoshimura et al., 2006; Kohzaki et al., 2010]. Another possible strategy is disruption of a gene responsible for excision-repair of UV-lesions in the $XPA^{-/-}$ background.

In this study, we also conducted a MN test using a $XPA^{-/-}$ cell line after exposure to four DNA damaging agents. As expected from the role of XPA in nucleotide excision repair but not in BER or SSB repair, $XPA^{-/-}$ cells showed no significant increases in MN induction in comparison with $wild$-$type$ cells upon exposure to H_2O_2 or MMS (Supporting Information, Fig. 6), which is in contrast with the prominent phenotypes in $RAD54^{-/-}/LIG4^{-/-}$ and $XRCC1^{-/-}$ cells (Fig. 3). Neither gamma rays nor MMC increased MN induction in $XPA^{-/-}$ cells in comparison with $wild$-$type$ cells.

After the identification of the genotoxicity of chemical compounds via in $vitro$ assay screening, molecular mechanisms underlying the genotoxicity may need to be clarified. The genotoxicity of chemicals is often caused by a few independent mechanisms. In fact, we previously revealed that sodium meta arsenite causes DNA damage through at least two different mechanisms, one depending on the formation of reactive-oxygen-species and the other being independent [Ji et al., 2009]. Thus, to understand mechanisms underlying the mutagenic potential of individual chemical compounds, we need to accurately quantitate the relative contribution of multiple DDR pathways to the repair of different types of lesions induced by each test chemical. Accurate quantitation may be a formidable challenge since the shape of dose response curves of cellular survival may distinctly differ depending on the DDR genes disrupted in mutant cells as well as on chemical compounds. In the current study, we simply compared the induced MN frequency between one of the mutant clones and $wild$-$type$ cells after exposure of these two clones to the same dose of DNA-damaging agents. While this protocol shows higher MN frequency of the isogenic mutants to typical DNA-damaging agents in the MN test, more time-consuming experimentation is required to accurately quantitate the relative contribution of multiple DDR pathways as we have done for DT40 isogenic mutants [Maede et al., 2014; Nishihara et al., 2016]. Thus, in the future, a practical MN protocol needs to be established to comprehensively investigate the molecular mechanisms underlying the genotoxicity, in addition to a MN protocol for simply identifying the genotoxic potential of test chemical compounds.

STATEMENT OF AUTHOR CONTRIBUTIONS

S.T. and L.K.S. designed the basic framework of this study. L.K.S performed all experiments with the help of S.K., S.A. and H.K. L.K.S. prepared the manuscript draft with intellectual input from S.T. J.N. and S.T. finalized the manuscript. T.S. and T.Y. provided information for designing some of the experiments. M.H. provided isogenic TK6 $wild$-$type$ cells. H.S and K.H advised L.K.S about technical issues during the experimentation. All authors have approved the final manuscript.

REFERENCES

Amundson SA, Do KT, Vinikoor L, Koch-Paiz CA, Bittner ML, Trent JM, Meltzer P, Fornace AJ. 2005. Stress-specific signatures: expression profiling of p53 wild-type and -null human cells. Oncogene 24:4572–4579.

Bradley MO, Kohn KW. 1979. X-ray induced DNA double strand break production and repair in mammalian cells as measured by neutral filter elution. Nucleic Acids Res 7:793–804.

Branzei D, Foiani M. 2010. Maintaining genome stability at the replication fork. Nat Rev Mol Cell Biol 11:208–219.

Cermak T, Doyle EL, Christian M, Wang L, Zhang Y, Schmidt C, Baller JA, Somia NV, Bogdanove AJ, Voytas DF. 2011. Efficient design and assembly of custom TALEN and other TAL effector-based constructs for DNA targeting. Nucleic Acids Res 39:7879

Couëdel C, Mills KD, Barchi M, Shen L, Olshen A, Johnson RD, Nussenzweig A, Essers J, Kanaar R, Li GC, Alt FW, Jasin M. 2004. Collaboration of homologous recombination and nonhomologous end-joining factors for the survival and integrity of mice and cells. Genes Dev 18:1293–1304.

Eppink B, Tafel AA, Hanada K, Drunen E, van, Hickson ID, Essers J, Kanaar R. 2011. The response of mammalian cells to UV-light reveals Rad54-dependent and independent pathways of homologous recombination. DNA Repair (Amst) 10:1095–1105.

Fellows MD, O'Donovan MR, Lorge E, Kirkland D. 2008. Comparison of different methods for an accurate assessment of cytotoxicity in the in vitro micronucleus test. II: Practical aspects with toxic agents. Mutat Res - Genet Toxicol Environ Mutagen 655:4–21.

Fukushima T, Takata M, Morrison C, Araki R, Fujimori A, Abe M, Tatsumi K, Jasin M, Dhar PK, Sonoda E, Chiba T, Takeda S. 2001. Genetic Analysis of the DNA-dependent Protein Kinase Reveals an Inhibitory Role of Ku in Late S-G2 Phase DNA Double-strand Break Repair. J Biol Chem 276:44413–44418.

Gibbs PEM, McDonald J, Woodgate R, Lawrence CW. 2005. The relative roles in vivo of Saccharomyces cerevisiae Pol eta, Pol zeta, Rev1 protein and Pol32 in the bypass and mutation induction of an abasic site, T-T (6-4) photoadduct and T-T cis-syn cyclobutane dimer. Genetics 169:575–582.

Goodarzi AA, Jeggo PA. 2013. The repair and signaling responses to DNA double-strand breaks. Adv Genet 82:1–45.

Greenwood SK, Armstrong MJ, Hill RB, Bradt CI, Johnson TE, Hilliard CA, Galloway SM. 1998. Fewer chromosome aberrations and earlier apoptosis induced by DNA synthesis inhibitors, a topoisomerase II inhibitor or alkylating agents in human cells with normal compared with mutant p53. MutatRes 401:39–53.

Greenwood SK, Hill RB, Sun JT, Armstrong MJ, Johnson TE, Gara JP, Galloway SM. 2004. Population Doubling: A Simple and More Accurate Estimation of Cell Growth Suppression in the in Vitro Assay for Chromosomal Aberrations that Reduces Irrelevant Positive Results. Environ Mol Mutagen 43:36–44.

Hastwell PW, Webster TW, Tate M, Billinton N, Lynch AM, Harvey JS, Rees RW, Walmsley RM. 2009. Analysis of 75 marketed pharmaceuticals using the GADD45a-GFP "GreenScreen HC" genotoxicity assay. Mutagenesis 24:455–463.

Hochegger H, Dejsuphong D, Fukushima T, Morrison C, Sonoda E, Schreiber V, Zhao GY, Saberi A, Masutani M, Adachi N, Koyama H, Murcia G. d, et al. 2006. Parp-1 protects homologous recombination from interference by Ku and Ligase IV in vertebrate cells. embo J 25:1305–1314.

Hochegger H, Sonoda E, Takeda S. 2004. Post-replication repair in DT40 cells: translesion polymerases versus recombinases. Bioessays 26:151–158.

Holthausen JT, Wyman C, Kanaar R. 2010. Regulation of DNA strand exchange in homologous recombination. DNA Repair (Amst) 9: 1264–1272.

Honma M, Hayashi M. 2011. Comparison of in vitro micronucleus and gene mutation assay results for p53-competent versus p53-deficient human lymphoblastoid cells. Environ Mol Mutagen 52: 373–384.

Horton JK, Watson M, Stefanick DF, Shaughnessy DT, Taylor JA, Wilson SH. 2008. XRCC1 and DNA polymerase β in cellular protection against cytotoxic DNA single-strand breaks. Cell Res 18:48–63.

Ji K, Kogame T, Choi K, Wang X, Lee J, Taniguchi Y, Takeda S. 2009. A novel approach using DNA-repair-deficient chicken DT40 cell lines for screening and characterizing the genotoxicity of environmental contaminants. Environ Health Perspect 117:1737–1744.

Keka IS, Mohiuddin, Maede Y, Rahman MM, Sakuma T, Honma M, Yamamoto T, Takeda S, Sasanuma H. 2015. Smarcal1 promotes double-strand-break repair by nonhomologous end-joining. Nucleic Acids Res 43:6359–6372.

Kim H, D'Andrea AD. 2012. Regulation of DNA cross-link repair by the Fanconi anemia/BRCA pathway. Genes Dev 26:1393–1408.

Kimura A, Miyata A, Honma M. 2013. A combination of in vitro comet assay and micronucleus test using human lymphoblastoid TK6 cells. Mutagenesis 28:583–590.

Kobayashi S, Kasaishi Y, Nakada S, Takagi T, Era S, Motegi A, Chiu RK, Takeda S, Hirota K. 2015. Rad18 and Rnf8 facilitate homologous recombination by two distinct mechanisms, promoting Rad51 focus formation and suppressing the toxic effect of nonhomologous end joining. Oncogene 34:4403–4411.

Kohzaki M, Nishihara K, Hirota K, Sonoda E, Yoshimura M, Ekino S, Butler JE, Watanabe M, Halazonetis TD, Takeda S. 2010. DNA polymerases nu and theta are required for efficient immunoglobulin V gene diversification in chicken. J Cell Biol 189:1117–1127.

Liber HL, Thilly WG. 1982. Mutation assay at the thymidine kinase locus in diploid human lymphoblasts. Mutat Res - Fundam Mol Mech Mutagen 94:467–485.

Maede Y, Shimizu H, Fukushima T, Kogame T, Nakamura T, Miki T, Takeda S, Pommier Y, Murai J. 2014. Differential and Common DNA Repair Pathways for Topoisomerase I- and II-Targeted Drugs in a Genetic DT40 Repair Cell Screen Panel. Mol Cancer Ther 13:214–220.

Mills KD, Ferguson DO, Essers J, Eckersdorff M, Kanaar R, Alt FW. 2004. Rad54 and DNA Ligase IV cooperate to maintain mammalian chromatid stability. Genes Dev 18:1283–1292.

Mizutani A, Okada T, Shibutani S, Sonoda E, Hochegger H, Nishigori C, Miyachi Y, Takeda S, Yamazoe M. 2004. Extensive Chromosomal Breaks Are Induced by Tamoxifen and Estrogen in DNA Repair-Deficient Cells. Cancer Res 64:3144–3147.

Mohiuddin M, Evans TJ, Rahman MM, Takeda S. 2018. SUMOylation of PCNA by PIAS1 and PIAS4 promotes template switch in vertebrate cells. Manuscript under revision in PNAS.

Murai J, Huang SYN, Das BB, Renaud A, Zhang Y, Doroshow JH, Ji J, Takeda S, Pommier Y. 2012. Trapping of PARP1 and PARP2 by clinical PARP inhibitors. Cancer Res 72:5588–5599.

Musich PR, Li Z, Zou Y. 2017. Xeroderma Pigmentosa Group A (XPA), Nucleotide Excision Repair and Regulation by ATR in Response to Ultraviolet Irradiation. Adv Exp Med Biol 996:41–54.

Nishihara K, Huang R, Zhao J, Shahane SA, Witt KL, Smith-Roe SL, Tice RR, Takeda S, Xia M. 2016. Identification of genotoxic compounds using isogenic DNA repair deficient DT40 cell lines on a quantitative high throughput screening platform. Mutagenesis 31:69–81.

OECD. 2014. OECD Guideline for the Testing of Chemicals TG 474 mammalian erythrocyte micronucleus test. 10.1787/9789264224292-en.

Olive PL, Frazer G, Banáth JP. 1993. Radiation-induced apoptosis measured in TK6 human B lymphoblast cells using the comet assay. Radiat Res 136:130–136.

Qing Y, Yamazoe M, Hirota K, Dejsuphong D, Sakai W, Yamamoto KN, Bishop DK, Wu X, Takeda S. 2011. The epistatic relationship between BRCA2 and the other RAD51 mediators in homologous recombination. PLoS Genet 7:e1002148

Ran FA, Hsu PD, Wright J, Agarwala V, Scott DA, Zhang F. 2013. Genome engineering using the CRISPR-Cas9 system. Nat Protoc 8:2281–2308.

Sakuma T, Ochiai H, Kaneko T, Mashimo T, Tokumasu D, Sakane Y, Suzuki K, Miyamoto T, Sakamoto N, Matsuura S, Yamamoto T. 2013. Repeating pattern of non-RVD variations in DNA-binding modules enhances TALEN activity. Sci Rep 3:3379

Sale JE, Lehmann AR, Woodgate R. 2012. Y-family DNA polymerases and their role in tolerance of cellular DNA damage. Nat Rev Mol Cell Biol 13:141–152.

Sonoda E, Sasaki MS, Buerstedde JM, Bezzubova O, Shinohara A, Ogawa H, Takata M, Yamaguchi-Iwai Y, Takeda S. 1998. Rad51-deficient vertebrate cells accumulate chromosomal breaks prior to cell death. embo J 17:598–608.

Takezawa J, Aiba N, Kajiwara K, Yamada K. 2011. Caffeine abolishes the ultraviolet-induced REV3 translesion replication pathway in mouse cells. Int J Mol Sci 12:8513–8529.

Wu X, Takenaka K, Sonoda E, Hochegger H, Kawanishi S, Kawamoto T, Takeda S, Yamazoe M. 2006. Critical roles for polymerase zeta in cellular tolerance to nitric oxide-induced DNA damage. Cancer Res 66:748–754.

Yamamoto KN, Hirota K, Kono K, Takeda S, Sakamuru S, Xia M, Huang R, Austin CP, Witt KL, Tice RR. 2011. Characterization of environmental chemicals with potential for DNA damage using isogenic DNA repair-deficient chicken DT40 cell lines. Environ Mol Mutagen 52:547–561.

Yatagai F, Suzuki M, Ishioka N, Ohmori H, Honma M. 2008. Repair of I-SceI Induced DSB at a specific site of chromosome in human cells: Influence of low-dose, low-dose-rate gamma-rays. Radiat Environ Biophys 47:439–444.

Yoshimura M, Kohzaki M, Nakamura J, Asagoshi K, Sonoda E, Hou E, Prasad R, Wilson SH, Tano K, Yasui A, Lan L, Seki M, et al. 2006. Vertebrate POLQ and POLbeta cooperate in base excision repair of oxidative DNA damage. Mol Cell 24:115–125.

Zhao GY, Sonoda E, Barber LJ, Oka H, Murakawa Y, Yamada K, Ikura T, Wang X, Kobayashi M, Yamamoto K, Boulton SJ, Takeda S. 2007. A Critical Role for the Ubiquitin-Conjugating Enzyme Ubc13 in Initiating Homologous Recombination. Mol Cell 25:663–675.

Accepted by—
S. Dertinger